Hexafluorobenzene in Comparison with Perfluoro-15-crown-5-ether for Repeated Monitoring of Oxygenation Using ^{19}F MRI in a Mouse Model

Lionel Mignion,[1] Julie Magat,[1] Olivier Schakman,[2] Etienne Marbaix,[3] Bernard Gallez,[1] and Bénédicte F. Jordan[1]*

Hexafluorobenzene (HFB) and perfluoro-15-crown-5-ether (15C5) were compared as fluorine reporter probes of tissue oxygenation using ^{19}F MRI for dynamic assessment of muscle oxygenation, with special focus on muscle tissue toxicity of the probes, and consecutive alteration of animal behavior. The latter were also compared in terms of sensitivity to changes in oxygenation as well as of signal-to-noise ratio for accurate pO_2 measurements. For that purpose, mouse muscles were imaged at 11.7 T, at 2- and 36-h after intramuscular injection of HFB or 15C5. Histological analysis of the muscle tissue revealed a lack of toxicity for 15C5 from 2 up to 36-h postinjection, whereas HFB induced tissue necrosis, blood clots and thrombosis as soon as 24-h postinjection. This muscle toxicity led to a limitation in mice mobility 24-h after injection of HFB as evidenced by behavioral testing (open-field, grip strength, and catwalk tests), which was not the case after 15C5 intramuscular injection. Finally, pO_2 measurements assessed 2-h postinjection showed consistent values with both probes, evidencing cross-validation of the ^{19}F MRI oximetry technique for acute measurements. However, the measurement at 36-h was hampered for HFB, which showed significant lower values of muscle pO_2, whereas 15C5 was able to reliably assess muscle pO_2 at 36-h postinjection. **Magn Reson Med 69:248–254, 2013.**

Key words: ^{19}F-MRI; oxygenation; HFB; 15C5

Hypoxia (deprivation of adequate oxygen supply) can have serious consequences on vascular disease, specific pulmonary disease, kidney disease, cardiovascular disease, stroke, and cancer, among others (1). In each case, lack of oxygen is associated with poor prognosis, and efforts are made to improve tissue oxygenation. Regarding cancer therapy, the efficacy of many therapeutic approaches to tumor treatment is known to be modulated by oxygen tension (2). Moreover, hypoxia is also associated with local recurrence or distant metastases in a variety of tumors (2). There is therefore a critical need to develop dynamic methods for direct oxygen mapping (2). The ideal technique would assess hypoxia in vivo, be minimally invasive and take into consideration the temporal and spatial heterogeneity of oxygenation.

A variety of oximetry techniques are proposed to assess hypoxia, which can be broadly categorized into direct and indirect measurements according to different principles and the ability to quantify tissue oxygenation (2). Indirect methods include blood oxygen level-dependent imaging and recent ^{1}H T_1-based magnetic resonance imaging (MRI) methods, positron emission tomography tracers retained in hypoxic regions, and near infrared spectroscopy (2). Methods to measure absolute pO_2 encompass invasive polarographic oxygen electrodes (Eppendorf system) and fluorescence quenching fiber-optic probes (OxyLite^{TM}), as well as electron paramagnetic resonance oximetry and ^{19}F relaxometry (2).

Fluorine MR uses perfluorocarbon (PFC) compounds to evaluate interstitial oxygen tension. Indeed, molecular oxygen dissolves in PFC and proportionately increases the relaxation rates of PFC (3). The technique allows ^{19}F MRI monitoring of the tissue oxygenation state and oxygen distribution in an organ (4). As there is a negligible endogenous ^{19}F MRI signal from the body, the lack of background signal provides ^{19}F MRI with a potentially extremely high contrast-to-noise ratio and specificity (5). Fluorine MRI, applied in the preclinical setting, is minimally invasive provided that PFC is not too toxic to surrounding tissues (6).

Different PFCs have been used for in vivo oxygenation studies, including perflubron (7), hexafluorobenzene (HFB) (8,9), oxypherol (10,11), and perfluoro-15-crown-5-ether (15C5) (12,13), among others. PFCs can be administered intravenously or directly by intratumoral injection of PFC droplets or emulsions (3).The group led by R. Mason initially developed the FREDOM fluorocarbon relaxometry using echo planar imaging for dynamic oxygen mapping technique (9), which has been applied to examine the effects of vasoactive agents (14), vascular targeting agents (15), as well as hyperoxic gases (16), and correlated with invasive direct in vivo or ex vivo methods (3). Our group also used intratumoral HFB for short-term (<2-h) dynamic monitoring of tumor oxygenation following hyperoxic challenges or spontaneous fluctuations in

[1]Biomedical Magnetic Resonance Group, Louvain Drug Research Institute, Université Catholique de Louvain, Brussels, Belgium.

[2]Laboratory of Cell Physiology, Institute of Neuroscience, Université Catholique de Louvain, Brussels, Belgium.

[3]Cell Biology Unit, de Duve Institute, Université Catholique de Louvain, Brussels, Belgium.

Contract grant sponsors: Belgian National Fund for Scientific Research (FNRS), Fonds Joseph Maisin, Saint-Luc Foundation, Actions de Recherche Concertées de la Communauté Française de Belgique-ARC 09/14-020, Pôle d'Attraction Interuniversitaire PAI VI (P6/38), Walloon Region's Marshall Programme of Excellence (DIANE convention).

*Correspondence to: Prof. Bénédicte F. Jordan, REMA, Avenue Mounier 73, boite B1.73.08, B-1200 Brussels, Belgium. E-mail: benedicte.jordan@uclouvain.be

Received 20 October 2011; revised 15 February 2012; accepted 17 February 2012.

DOI 10.1002/mrm.24245

Published online 22 March 2012 in Wiley Online Library (wileyonlinelibrary.com).

tumor models, using a Look Locker approach in order to achieve a better temporal resolution than FREDOM (17,18).

Even though PFCs are described as chemically inert and stable compounds (19), our group observed long-term tissue toxicity effects using HFB, which hampers its use for chronic studies. The molecule 15C5, with 20 fluorine atoms, presents a high signal-to-noise ratio and has been applied in chronic studies (12). The aim of the current study was therefore to compare HFB with 15C5 in terms of ability to assess physiological pO_2 in muscle, as well as in terms of potential muscle tissue toxicity and alteration of mouse behavior.

METHODS

Animals and Products

Male NMRI mice (Elevage Janvier, France) were used for MRI experiments and PFC injections. Animals were anesthetized by inhalation of isoflurane (induction: 3%; maintenance 1.5%) delivered by a nose cone. HFB (Fluka, Sigma-Aldrich, United States) and 15C5 (Fluorochem, United Kingdom) were injected into the muscle of the right hind paw using a syringe with a 29G needle and deposited along three tracks (3 × 30 μL) encompassing both central and peripheral regions.

Histology

HFB or 15C5 was injected into the muscle of the right hind paw of 10 mice. After 0.5, 2, 4, 24, and 36 h, one mouse with HFB and one with 15C5 were sacrificed. The intact muscle tissue was dissected and stored in 4% paraformaldehyde overnight. The fixed muscle was paraffin-embedded and sliced into 5 μm sections encompassing the muscle injection site. Alternate sections were stained with hematoxylin and eosin and imaged using a microscope.

Behavioral Testing

All the behavioral tests were performed 24-h after intramuscular injection of 15C5 or HFB.

Open-Field Test [15C5 (n = 6) and HFB (n = 5)]

The open-field test was used to assess a nonforced ambulation as mice can move freely without any influence of the examiner. Briefly, mice were placed in a square arena (60 × 60 cm^2) and video tracked (Ethovision 6.1, Noldus; Wageningen, The Netherlands) for 20 min (20). The total distance covered by the animals, the proportion of time during which each animal moved and the average speed of movement were measured.

Grip Strength Test [15C5 (n = 6) and HFB (n = 5)]

The grip strength test was used to measure the strength of combined fore limb-hindlimb muscles. Limb strength was recorded using a grid connected to a sensor (Panlab-Bioseb, Vitrolle, France). Mice were gently laid on the top of the grid so that both their front paws and hind paws could grip the grid. They were then pulled back steadily until the grip was released down the complete length of the grid (20). Two series of three tests were performed at an interval of 15 min. Results are presented as the mean of the two highest values of force recorded, related to body weight.

Catwalk test [15C5 (n = 6) and HFB (n = 4)]

The Catwalk test was used to assess the gait of voluntarily walking mice (Catwalk 7, Noldus; Wageningen, The Netherlands) (21). Paw print recording allowed analysis of various aspects of walking steps such as the basis of support, the pressure of the paws on the floor, the length of contact and the sequence regularity of steps (22). Five runs were performed per animal and analysis was performed on the fastest uninterrupted run.

The mice were weighed daily over a 4-day period after the PFC injections (day 1 corresponding to 24-h postinjection of the probes).

^{19}FMRI Acquisitions

MRI was performed with an 11.7 T, 16 cm inner diameter bore system (Bruker Biospec, Ettlingen, Germany) equipped for respiration and temperature monitoring. Mouse temperature was maintained at 37°C ± 0.5°C by using a water blanket connected to a circulating water bath. A tunable ^{1}H/^{19}F surface coil was used for radiofrequency transmission and reception. Adjustments (shimming, geometry) were performed at the proton frequency (500 MHz), and then scans were acquired using the fluorine frequency (470 MHz).

MRI scout images were obtained for both ^{1}H and ^{19}F to reveal HFB or 15C5 distribution within the muscle. A polygonal region of interest (ROI) in muscle was defined and a nonlinear fit was used to determine the T_1 relaxation in each pixel of the ROI. We then used a segmented FISP (Fast Imaging with Steady state Precession) sequence in FID mode to acquire ^{19}F images of T_1 relaxation times of HFB and 15C5 distributions. The acquisition parameters were TR/TE/FA/BW/NA/matrix = 4 ms/1.2 ms/5°/100 kHz/2/64 × 64, four segments, and a total acquisition time of 1 min 36 s. In order to sample the recovery of the signal, a series of 100 images are acquired between 30 and 9930 ms (TR = 100 ms between segments) with a slice thickness of 10 mm. Images were then treated using a homemade program written in Matlab to determine the T_1 relaxation (in ms) in regions of interest and convert it into pO_2 values.

Calibration of HFB (R_1 with respect to pO_2) was performed at 11.7 T and at 37°C ± 0.5°C by measuring R_1 in sealed tubes (n = 2) containing 300 μL HFB consecutively bubbled with nitrogen (0% O_2 = 0 mmHg), air (21% O_2 = 160 mmHg), and carbogen (95% O_2 = 722 mmHg) for 20 min in a 37°C ± 0.5°C water bath before measurement.

For 15C5, a 10% w/v PFC emulsion with a pH of 7.22 and an isotonicity of 300 mOsm/kg was used for calibration (23). The composition of the emulsion was 10% PFC, 3% w/v purified egg lecithin, 1.8% glycerin and 18.7 mM phosphate buffer. Calibration measurements (n = 4) were then performed similarly to the procedure described for HFB.

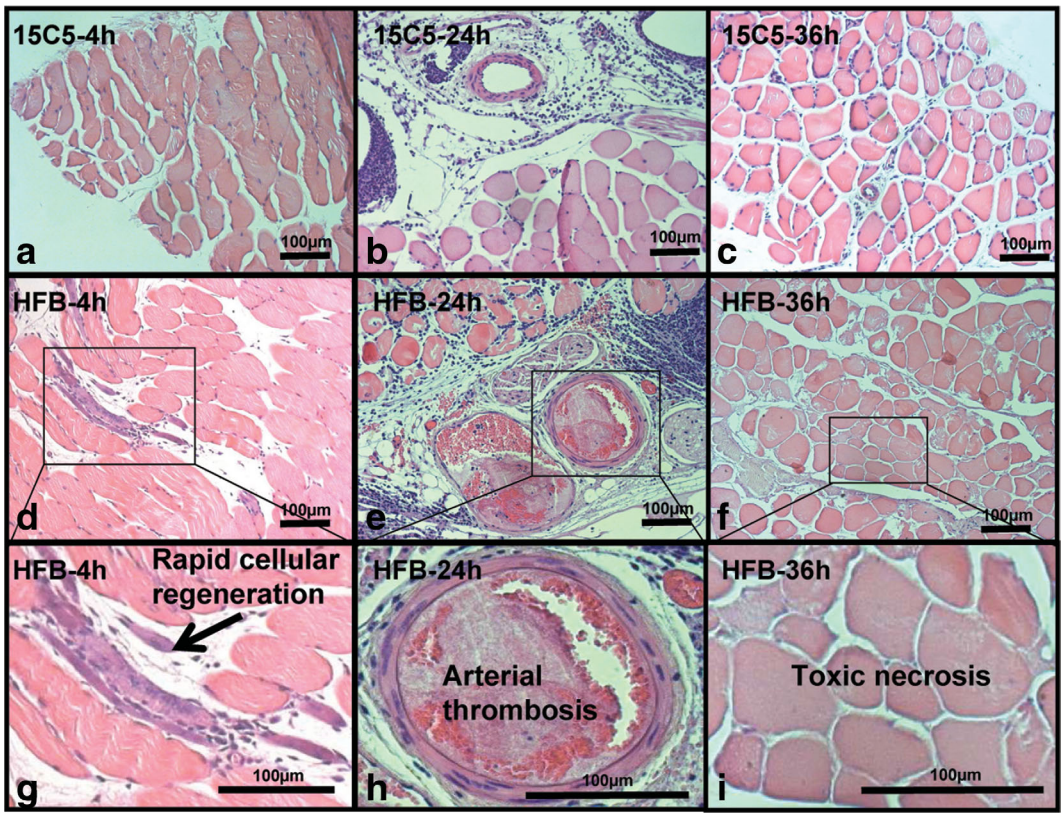

FIG. 1. Microscopic toxicity of HFB and 15C5. (**a–c**) Histological muscle sections at 4-h (a), 24-h (b), or 36-h (c) post 15C5 intramuscular injection, showing that the muscle tissue is not altered and presents only some inflammatory infiltrates. (**d–f**) Histological muscle sections at 4-h (d), 24-h (e), or 36-h (f) post HFB intramuscular injection, showing rapid cellular regeneration in muscle and inflammatory infiltrates (d), and the presence of thrombus (e) and toxic necrosis (f) as soon as 24-h postinjection. (**g–i**) Magnification of areas shown on d, e, and f.

A multiple linear least-squares regression was used to find the dependence of R_1 on dissolved oxygen for both HFB and 15C5. The correlation between T_1 (s) and pO_2 (mmHg) was used to obtain a map of the partial oxygen pressure for each voxel. The physiologically relevant data from 0 to 160 mmHg were used in our analysis.

Statistical Data Analysis

Results are presented as means± standard deviation and paired *t*-tests were conducted on these results, with $P < 0.05$ being considered as significant. Two-way ANOVA with Bonferonni post hoc test was used to compare the weight loss over time between HFB and 15C5 mice.

RESULTS

Effect of HFB and 15C5 on Muscle Tissue Histology

Microscopic effects of HFB and 15C5 were compared at 4-, 24-, and 36-h after intramuscular injection in the right hind paw (Fig. 1). At 2-h after injection of 15C5 or HFB, the muscle tissue was not modified, with only small inflammatory infiltrates near the injection sites. We observed rapid cellular regeneration in muscle as soon as 4-h after HFB injection, which was not the case for 15C5 (Fig. 1a,d). At 24- and 36-h after HFB injection, toxic necrosis in muscular tissue was present, along with blood clots in vessels leading to thrombosis (Fig. 1e,f). After 15C5 injection, the muscular tissue had no modified morphology at any time point, with only some inflammatory infiltrates (Fig. 1b,c).

Effect of HFB and 15C5 on Mice Behavior

General activity, measured in the open-field test, was systematically higher for mice injected with 15C5 than for mice injected with HFB. The total distance covered by mice injected with 15C5 was longer (9634 ± 1492 cm) than for mice injected with HFB(2356 ± 1592 cm; $P < 0.0001$). The 15C5 mice were also more often in movement (71 ± 5 % vs. 21 ± 16% of the total time, $P < 0.0001$; Fig. 2a) and moved faster (8 ± 1 cm/s) than mice injected with HFB (2 ± 1 cm/s, $P < 0.0001$; Fig. 2a).

For the grip test, a sensitive gauge recorded the peak force applied by each animal. The force developed by mice injected with 15C5 was higher with 15C5 (7.5 ± 0.6) than for mice injected with HFB (6 ± 0.9, $P < 0.01$; Fig. 2b).

On the catwalk test, we observed a higher speed of locomotion crossing the runway for mice injected with 15C5 (34 ± 4 cm/s) than for mice injected with HFB (20 ± 2 cm/s, $P < 0.0001$; Fig. 2c). The duration of contact of the injected paw with the ground was also significantly higher with 15C5 (72.5 ± 3.9 % vs. 26.4 ± 11.6 %, $P < 0.0001$; Fig. 2c) and the area of contact with the ground was larger with this product (31.3 ± 7.6 mm^2 versus 1.1 ± 0.8 mm^2, $P < 0.0001$; Fig. 2c).

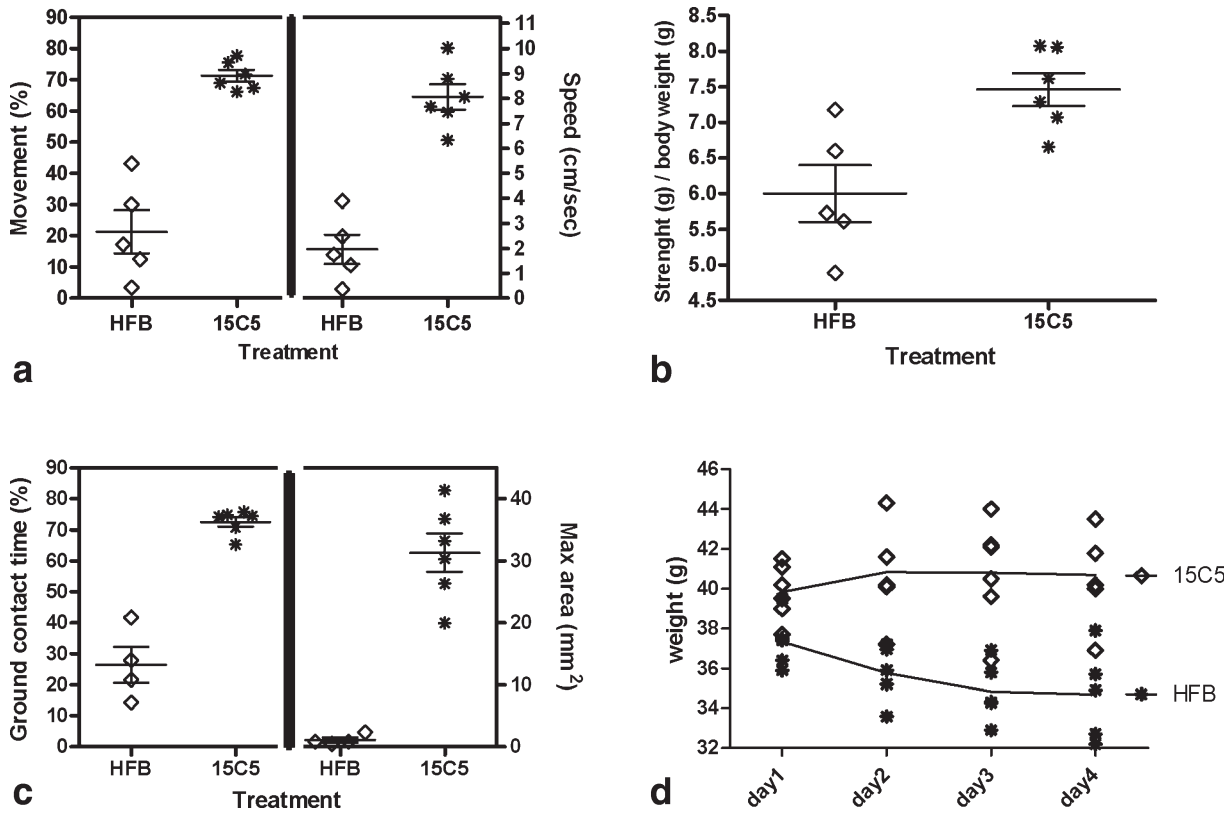

FIG. 2. Comparison of HFB and 15C5 mice behavior: (**a**) Open-field to measure exploration activity; (**b**) Grip test to measure muscular strength; (**c**) Catwalk test to analyze ground contact of the injected paw; and (**d**) Mice weight. In a, b, c, means +/− standard errors are shown; in d, the lines join the means of each group.

Finally, mice's weight was recorded daily over a 4-day period after injection, all mice having the same origin and age. With HFB, we observed a decrease in the mice's weight, whereas the weight of 15C5 mice was stable after injections (Fig. 2d; $P < 0.001$ at day 2, 3, 4 while comparing HFB and 15C5 groups; two-way ANOVA).

Ability of HFB and 15C5 to Assess Muscle Oxygenation with ^{19}F-MRI

PFC Calibrations

The effective pO_2 was determined by measuring the ^{19}F T_1 of 15C5 emulsion or HFB solution versus dissolved oxygen concentration for three different oxygen tensions. Figure 3 shows the calibration curves measured at 11.7 T and 37°C ± 0.5°C for HFB and 15C5, respectively. Using linear regression analyses, we obtained the relationship between R_1 (= $1/T_1$) and pO_2 given by: [R_1 = 0.00303 (pO_2) + 0.63639] for HFB and [R_1 = 0.0063 (pO_2) + 1.7447] for 15C5, where R_1 and pO_2 have units of s^{-1} and mmHg.

Sensitivity Index and Signal-to-Noise Ratio

The calculated sensitivity indexes (representing the sensitivity of each probe to changes in oxygenation), defined as b/a (=slope/intercept) in an $R = ax + b$ calibration curve (3), are 0.00476 for HFB and 0.00361 for 15C5, at 11.7 T, 15C5 (25% less sensitive). However, thanks to its higher number of fluorine atoms and its higher density (15C5 vs. HFB: 20 vs. six fluorine atoms and 1.78 vs. 1.61 g/mL), 15C5 presented a S/N ratio of ∼40 for 15C5 (at 2- and 36-h postinjection), whereas HFB showed a S/N ratio of ∼20 at 2-h postinjection and of ∼6 at 36-h postinjection, illustrating the loss of signal over time (Fig. 4). Overall, taking into account the slightly lower sensitivity of 15C5 and its higher (double) S/N ratio, our analysis resulted in a mean of 40 pixels analyzed (being correctly fitted with a T_1 error/$T_1 < 30\%$) in muscles at 2-h postinjection of 15C5 ($n = 4$/group) vs. 27 pixels for HFB ($n = 4$/group). At 36-h, the number of pixels analyzed was significantly reduced for HFB but not for 15C5 (91 pixels analyzed for 15C5 and 13 pixels for HFB at 36-h).

Measurement of Muscle Oxygenation Using HFB and 15C5

HFB or 15C5 were injected in mouse muscle ($n = 4$ for HFB and 15C5). Muscles were imaged using ^{19}F MRI at 2- and 36-h postinjection. Two hours after injection of PFC, pO_2 was similar in both groups of mice (Fig. 5). At 36-h postinjection, the HFB mice showed a decrease in muscular pO_2 ($P < 0.05$; Fig. 5), whereas the 15C5 mice were stable and did not show any significant change in pO_2 between 2- and 36-h. The apparent decrease in muscle pO_2 using HFB could be due to the modification of muscle tissue histology as well as to the selective retention of the probe in less well perfused regions (which are therefore also more hypoxic), while being washed out from well perfused regions.

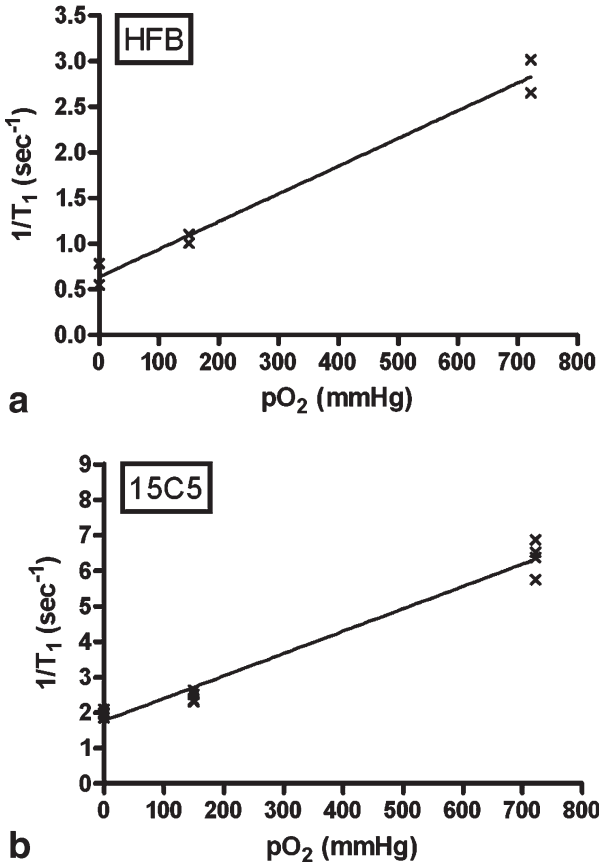

FIG. 3. Calibration curves of R_1 ($1/T_1$) versus pO_2 (mmHg) for HFB (**a**) and 15C5 (**b**), at 11.7 T (37°C).

DISCUSSION

A method for directly monitoring the heterogeneous distribution of partial oxygen pressure is the linear increase of the longitudinal relaxation rate ($1/T_1$) of PFCs with increasing pO_2 (3). Vascular delivery of PFC has been shown to favor delivery to well perfused and hence well oxygenated regions (10). Thus the most effective approach that has been suggested to achieve representative interrogation of a tumor is direct intratumoral delivery of the reporter molecules (3). The aim of the current study was to compare the ability of two PFCs, namely HFB and 15C5, to assess muscle tissue oxygenation and to compare their effects in terms of tissue toxicity, sensitivity, and signal-to-noise ratio.

The two PFCs used in this study are highly sensitive to pO_2, present a high signal-to-noise ratio, a single narrow spectral peak, and a linear relationship across the entire range of oxygenation. Since 15C5 is more sensitive to temperature (3.0 mmHg/°C) (3) than HFB (0.1 mmHg/°C) (3), it is critical to closely monitor animal temperature as well as in vitro samples to generate calibration data. In addition, the sensitivity of 15C5 is 25% lower than HFB at 11.7 T. However, this effect was more important at lower magnetic fields, as described by others: at 4.7 T, HFB presented a sensitivity index of ~0.02 vs. ~0.005 for 15C5 (four times less sensitive; Table 1). An important advantage of 15C5 over HFB, however, is its longer half-life and higher number of fluorine atoms, resulting in a higher signal-to-noise ratio that allows daily measurements without additional injection of the probe, contrary to HFB, which provides less signal 24- or 48-h after injection (as illustrated in Fig. 4). Zhao et al. showed in their study (15) that additional doses of HFB are required for the 24-h follow-up study of pO_2 for the control tumor group. For these control tumors, no significant differences in pO_2 were found with HFB in any of the measurements (immediately after HFB injection or 24-h after) (15).

It has been reported that HFB exhibits no mutagenicity or teratogenicity (19) and clears from the body rapidly owing to its highly volatile nature (within 24 h). HFB has been used in many species including cats, dogs, rats and mice, among others (3). However, to our knowledge, no study has focused on the tissue toxicity of HFB for "chronic" monitoring of tissue oxygenation (>2-h). At 2-h postinjection of the probes, the muscle tissue was unaltered with 15C5 as well as with HFB. However, the histological analysis of the muscle tissue showed modifications as soon as 4-h after injection of HFB, contrary to 15C5. We show here that injection of HFB in muscle causes a toxic necrosis with thrombosis in vessels 24-h after injection, a toxicity that is not present with 15C5. For this reason, the use of HFB to assess physiological measurement of pO_2 in a tissue should be limited to a maximum of 2-h postinjection. Moreover, the half-life of HFB in poorly perfused organs is reported to be ~10-h or less in the more vascularized organs, which makes daily monitoring of pO_2 difficult without additional injection of the probe (28), thereby generating even more tissue toxicity and bias in pO_2 measurements. We show here that 15C5 is more adapted to chronic experiments since the probe does not induce tissue toxicity (as is the case for a physiologic liquid injection that shows only a small inflammatory reaction at the site of injection). pO_2 measurements assessed 2-h postinjection showed consistent values with both probes, evidencing cross-validation of the ^{19}F MRI oximetry technique for acute measurements. However, the measurement at 36-h was hampered for HFB, which showed significantly lower values of muscle pO_2, whereas 15C5 was able to reliably assess muscle pO_2 at 36-h postinjection. The apparent decrease in muscle pO_2 using HFB is likely to be due to the modification of muscle tissue histology as well as to the selective

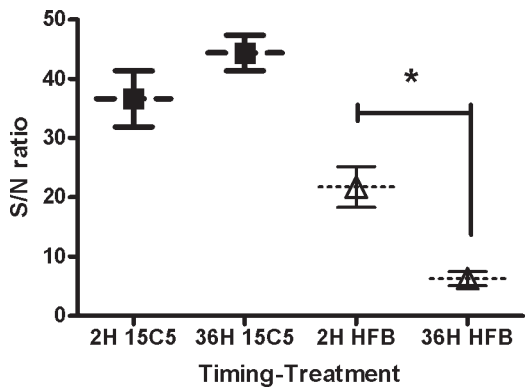

FIG. 4. Evolution of signal-to-noise (S/N) ratio for 15C5 and HFB at 2- and 36-h postinjection of the probes.

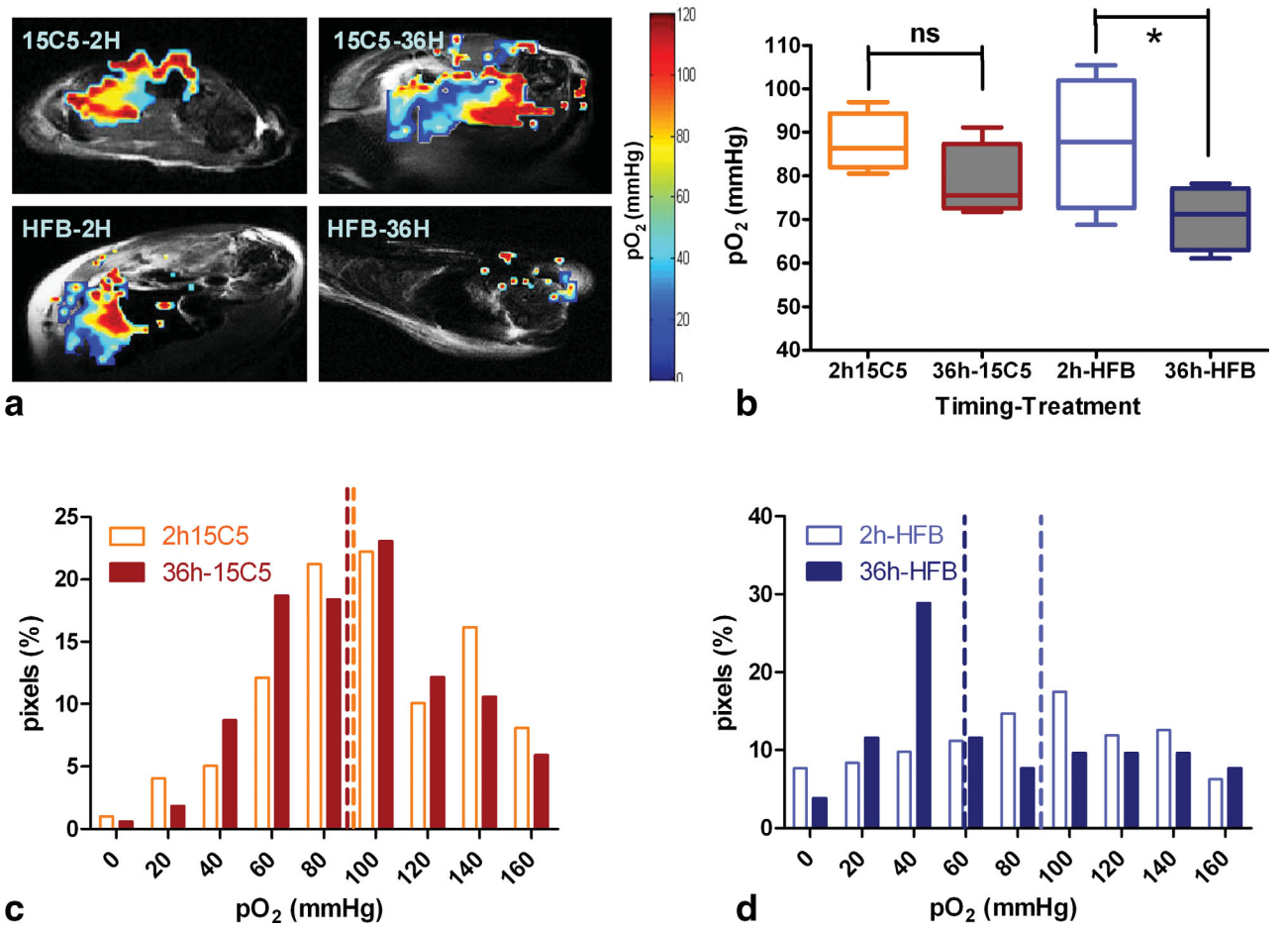

FIG. 5. Muscle pO_2 measurements at 2- and 36-h postinjection. (**a**) Typical maps of pO_2 values in the muscle measured with ^{19}F MR relaxometry, (**b**) Boxplot graph showing the evolution of mean pO_2 after HFB and 15C5 intramuscular injections, (**c**,**d**) Typical frequency distributions of pO_2 values using 15C5 or HFB at 2- and 36-h postinjection, respectively (dotted lines indicate the corresponding median values).

retention of the probe in less well perfused regions. In addition, using multiple tests, we observed that the intramuscular injection of HFB was able to influence mice behavior as soon as 24-h after injection. Indeed, mice injected with HFB did not use the injected paw in an optimal way, whereas 15C5 mice presented normal displacement. The weight loss and decrease of exploration behavior of the mice demonstrate the toxicity of HFB 24-h postinjection.

Table 1
Sensitivity Indexes for HFB and 15C5 at Different Magnetic Fields

PFC	Magnetic field (T)	Sensitivity index B/A	References
HFB	4,7	0.0225	9
	4.7	0.0225	24
	4.7	0.0191	17
	7	0.0159	4
	11.7	0.0048	This study
15C5	2	0.0099	25
	2	0.0099	12
	4.3	0.0064	16
	4.7	0.0059	26
	4.7	0.0053	27
	9.4	0.0043	26
	11.7	0.0036	This study

Most of the previously published studies using HFB were 'acute' studies with either similar doses of HFB (17) or even lower doses of HFB (8), and showed consistent monitoring of tissue pO_2. Our ^{19}F MRI oximetry values are in line with the recently published results of Liu et al. (4), who studied the level of oxygenation of different organs and tissues in rats using fluorine relaxometry along with HFB probe. However, these values are higher than those usually obtained with other direct techniques in skeletal muscle in rodents, including electron paramagnetic resonance (29–31), the Eppendorf system (32,33), or OxyLite probes (17). Nevertheless, the use of the technique for individual monitoring or comparison between groups has found broad applications in the preclinical field, and yet remains a unique minimally invasive technique for direct monitoring of tissue oxygenation.

CONCLUSIONS

In summary, even though ^{19}F MRI oximetry technique provides a sensitive method for measuring regional organ tissue oxygen tension and dynamic changes, it is important

to use an appropriate probe for chronic measurements. Indeed, the use of HFB as a reporter probe is mostly applicable for acute measurements (<2-h). We did show that 15C5 is better suited to chronic measurements of pO_2 with ^{19}F MRI, since it presents a lack of tissue toxicity and impact on animal behavior, and because of its longer half life and signal-to-noise ratio that does not imply repeated injections of the probe. Acute pO_2 measurements showed consistent values with both probes, evidencing cross-validation of the ^{19}F MRI oximetry technique for that purpose. However, the measurement at 36-h was hampered for HFB, which showed significant lower values of muscle pO_2, whereas 15C5 was able to reliably assess muscle pO_2 at 36-h postinjection.

ACKNOWLEDGMENTS

LM is "Télévie" Researcher and BFJ is a Research Associate of the Belgian National Fund for Scientific Research

REFERENCES

1. Gassmann M. Hypoxia, from Integrative biology to human disease. High Altitude Med Biol 2008;9:100–101.
2. Tatum JL, Kelloff GJ, Gillies RJ, Arbeit JM, Brown JM, Chao KS, Chapman JD, Eckelman WC, Fyles AW, Giaccia AJ, Hill RP, Koch CJ, Krishna MC, Krohn KA, Lewis JS, Mason RP, Melillo G, Padhani AR, Powis G, Rajendran JG, Reba R, Robinson SP, Semenza GL, Swartz HM, Vaupel P, Yang D, Croft B, Hoffman J, Liu G, Stone H, Sullivan D. Hypoxia: importance in tumor biology, noninvasive measurement by imaging, and value of its measurement in the management of cancer therapy. Int J Radiat Biol 2006;82:699–757.
3. Yu JX, Cui W, Zhao D, Mason RP. Non-invasive physiology and pharmacology using ^{19}F Magnetic Resonance. In: Tressaud A, Haufe G, editors. Fluorine and Health: Molecular Imaging, Biomedical Materials and Pharmaceuticals. Oxford, UK: Elsevier Science & Technology; 2008. 197–276.
4. Liu S, Shah SJ, Wilmes LJ, Feiner J, Kodibagkar VD, Wendland MF, Mason RP, Hylton N, Hopf HW, Rollins MD. Quantitative tissue oxygen measurement in multiple organs using (19) F MRI in a rat model. Magn Reson Med 2011;66:1722–1730.
5. Ruiz-Cabello J, Barnett BP, Bottomley PA, Bulte JWM. Fluorine (19F) MRS and MRI in biomedicine. NMR Biomed 2011;24:114–129.
6. Mason RP, Zhao D, Pacheco-Torres J, Cui W, Kodibagkar VD, Gulaka PK, Hao G, Thorpe P, Hahn EW, Peschke P. Multimodality imaging of hypoxia in preclinical settings. Q J Nucl Med Mol Imaging 2010; 54:259–280.
7. Tran HT, Guo Q, Schumacher DJ, Buxton RB, Mattrey RF. 19F chemical shift imaging technique to measure intracellular pO_2 in vivo using perflubron. Acad Radiol 1995;2:756–761.
8. Le D, Mason RP, Hunjan S, Constantinescu A, Barker BR, Antich PP. Regional tumor oxygen dynamics: 19F PBSR EPI of hexafluorobenzene. Magn Reson Imaging 1997;15:971–981.
9. Hunjan S, Zhao D, Constantinescu A, Hahn EW, Antich PP, Mason RP. Tumor oximetry: demonstration of an enhanced dynamic mapping procedure using fluorine-19 echo planar magnetic resonance imaging in the Dunning prostate R3327-AT1 rat tumor. Int J Radiat Oncol Biol Phys 2001;49:1097–1108.
10. Mason RP, Antich PP, Babcock EE, Constantinescu A, Peschke P, Hahn EW. Non-invasive determination of tumor oxygen tension and local variation with growth. Int J Radiat Oncol Biol Phys 1994;29:95–103.
11. Baldwin NJ, Ng TC. Oxygenation and metabolic status of KHT tumors as measured simultaneously by 19F magnetic resonance imaging and 31P magnetic resonance spectroscopy. Magn Reson Imaging 1996;14:541–551.
12. Dardzinski BJ, Sotak CH. Rapid tissue oxygen tension mapping using 19F inversion-recovery echo-planar imaging of perfluoro-15-crown-5-ether. Magn Reson Med 1994;32:88–97.
13. Nöth U, Rodrigues LM, Robinson SP, Jork A, Zimmermann U, Newell B, Griffiths JR. In vivo determination of tumor oxygenation during growth and in response to carbogen breathing using 15C5-loaded alginate capsules as fluorine-19 magnetic resonance imaging oxygen sensors. Int J Radiat Oncol Biol Phys 2004;60:909–919.
14. Zhao D, Constantinescu A, Jiang L, Hahn EW, Mason RP. Prognostic radiology: quantitative assessment of tumor oxygen dynamics by MRI. Am J Clin Oncol 2001;24:462–466.
15. Zhao D, Jiang L, Hahn EW, Mason RP. Tumor physiological response to combretastatin A4 phosphate assessed by MRI. Int J Radiat Oncol Biol Phys 2005;62:872–880.
16. van der Sanden BP, Heerschap A, Hoofd L, Simonetti AW, Nicolay K, van der Toorn A, Colier WN, van der Kogel AJ. Effect of carbogen breathing on the physiological profile of human glioma xenografts. Magn Reson Med 1999;42:490–499.
17. Jordan BF, Cron GO, Gallez B. Rapid monitoring of oxygenation by 19F magnetic resonance imaging: simultaneous comparison with fluorescence quenching. Magn Reson Med 2009;61:634–638.
18. Magat J, Jordan BF, Cron GO, Gallez B. Noninvasive mapping of spontaneous fluctuations in tumor oxygenation using 19F MRI. Med Phys 2010;37:5434–5441.
19. Courtney KD, Andrews JE. Teratogenic evaluation and fetal deposition of hexabromobenzene (HBB) and hexafluorobenzene (HFB) in CD-1 mice. J Environ Sci Health B 1984;19:83–94.
20. Mallon A-M, Blake A, Hancock JM. EuroPhenome and EMPReSS: online mouse phenotyping resource. Nucleic Acids Res 2008;36: 715–718.
21. Angeby-Möller K, Berge O-G, Hamers FPT. Using the CatWalk method to assess weight-bearing and pain behaviour in walking rats with ankle joint monoarthritis induced by carrageenan: effects of morphine and rofecoxib. J Neurosci Methods 2008;174:1–9.
22. Vandeputte C, Taymans J-M, Casteels C, Coun F, Ni Y, Van Laere K, Baekelandt V. Automated quantitative gait analysis in animal models of movement disorders. BMC Neurosci 2010;11:92:1–11.
23. McNab JA, Yung AC, Kozlowski P. Tissue oxygen tension measurements in the Shionogi model of prostate cancer using 19F MRS and MRI. MAGMA 2004;17:288–295.
24. Hunjan S, Mason RP, Constantinescu A, Peschke P, Hahn EW, Antich PP. Regional tumor oximetry: 19F NMR Spectroscopy of Hexafluorobenzene. Int J Radiat Oncol Biol Phys 1998;41:161–171.
25. Helmer KG, Han S, Sotak CH. On the correlation between the water diffusion coefficient and oxygen tension in RIF-1 tumors. NMR Biomed 1998;11:120–130.
26. Duong TQ, Iadecola C, Kim SG. Effect of hyperoxia, hypercapnia, and hypoxia on cerebral interstitial oxygen tension and cerebral blood flow. Magn Reson Med 2001;45:61–70.
27. Fan X, River JN, Zamora M, Al-Hallaq HA, Karczmar GS. Effect of carbogen on tumor oxygenation: combined fluorine-19 and proton MRI measurements. Int J Radiat Oncol Biol Phys 2002;54:1202–1209.
28. Zhao D, Jiang L, Mason RP. Measuring changes in tumor oxygenation. Meth Enzymol 2004;386:378–418.
29. Matsumoto S, Espey MG, Utsumi H, Devasahayam N, Matsumoto K, Matsumoto A, Hirata H, Wink DA, Kuppusamy P, Subramanian S, Mitchell JB, Krishna MC. Dynamic monitoring of localized tumor oxygenation changes using RF pulsed electron paramagnetic resonance in conscious mice. Magn Reson Med 2008;59:619–625.
30. Jordan BF, Kimpalou JZ, Beghein N, Dessy C, Feron O, Gallez B. Contribution of oxygenation to BOLD contrast in exercising muscle. Magn Reson Med 2004;52:391–396.
31. Aragonés J, Schneider M, Van Geyte K, Fraisl P, Dresselaers T, Mazzone M, Dirkx R, Zacchigna S, Lemieux H, Jeoung NH, Lambrechts D, Bishop T, Lafuste P, Diez-Juan A, Harten SK, Van Noten P, De Bock K, Willam C, Tjwa M, Grosfeld A, Navet R, Moons L, Vandendriessche T, Deroose C, Wijeyekoon B, Nuyts J, Jordan B, Silasi-Mansat R, Lupu F, Dewerchin M, Pugh C, Salmon P, Mortelmans L, Gallez B, Gorus F, Buyse J, Sluse F, Harris RA, Gnaiger E, Hespel P, Van Hecke P, Schuit F, Van Veldhoven P, Ratcliffe P, Baes M, Maxwell P, Carmeliet P. Deficiency or inhibition of oxygen sensor Phd1 induces hypoxia tolerance by reprogramming basal metabolism. Nat Genet. 2008;40:170–180.
32. Mason RP, Hunjan S, Constantinescu A, Song Y, Zhao D, Hahn EW, Antich PP, Peschke P. Tumor oximetry: comparison of ^{19}F MR EPI and electrodes. Adv Exp Med Biol 2003;530:19–27.
33. Eu JP, Hare JM, Hess DT, Skaf M, Sun J, Cardenas-Navina I, Sun QA, Dewhirst M, Meissner G, Stamler JS. Concerted regulation of skeletal muscle contractility by oxygen tension and endogenous nitric oxide. Proc Natl Acad Sci USA 2003;100:15229–15234.